

# Aerosol and Dimethyl Sulfide Sensitivity to Sulfate Chemistry Schemes

Yusuf A. Bhatti<sup>1</sup>, Laura E. Revell<sup>1</sup>, Adrian J. McDonald<sup>1</sup>, Alex T. Archibald<sup>2,3</sup>, Alex J. Schuddeboom<sup>1,\*</sup>, Jonny Williams<sup>4</sup>, Catherine Hardacre<sup>5,#</sup>, Jane Mulcahy<sup>5</sup>, Dongqi Lin<sup>6</sup>

<sup>1</sup>School of Physical and Chemical Sciences, University of Canterbury, Christchurch, New Zealand

<sup>2</sup>National Centre for Atmospheric Science, Cambridge, United Kingdom

<sup>3</sup>Yusuf Hamied Department of Chemistry, University of Cambridge, Cambridge, United Kingdom

<sup>4</sup>National Institute of Water and Atmospheric Research (NIWA), Wellington, New Zealand

<sup>5</sup>Met Office, Exeter, EX1 3PB, United Kingdom

<sup>6</sup>School of Earth and Environment, University of Canterbury, Christchurch, New Zealand

\*Now at National Institute of Water and Atmospheric Research (NIWA), Christchurch, New Zealand

#Now at School of Physical and Chemical Sciences, University of Canterbury, Christchurch, New Zealand

## Key Points:

- Seven DMS and sulfate chemistry schemes are tested in a single global climate model.
- The simulated spread in AOD and CDNC is more than twice as large as the change from pre-industrial to present-day.
- Constraining the chemistry of atmospheric sulfur is critical to constrain aerosol-cloud interactions.

---

Corresponding author: Yusuf Bhatti, [yusuf.bhatti@pg.canterbury.ac.nz](mailto:yusuf.bhatti@pg.canterbury.ac.nz)

## Abstract

Dimethyl sulfide (DMS) is the largest source of natural sulfur in the atmosphere and undergoes oxidation reactions resulting in gas-to-particle conversion to form sulfate aerosol. Climate models typically use independent chemical schemes to simulate these processes, however, the sensitivity of sulfate aerosol to the schemes used by CMIP6 models has not been evaluated. Here, we implemented seven DMS and sulfate chemistry schemes in an atmosphere-only Earth system model. A large spread in aerosol optical depth (AOD) is simulated (0.077), almost twice the magnitude of the pre-industrial to present-day increase in AOD. Differences are largely driven by the inclusion of the nighttime DMS oxidation reaction with  $\text{NO}_3$ , and in the number of aqueous phase sulfate reactions. Our analysis identifies the importance of DMS-sulfate chemistry for simulating aerosols. We suggest that optimizing DMS/sulfur chemistry schemes is crucial for the accurate simulation of sulfate aerosols.

## Plain Language Summary

Dimethyl sulfide (DMS) is a sulfur-bearing gas predominantly emitted from marine biological activity. DMS is the largest natural contributor to the global sulfur cycle, but its contribution is highly uncertain. Representing the complex chemical conversion of DMS to form natural sulfur atmospheric particles accurately in Earth System Models is difficult. Complex atmospheric chemistry is expensive to implement, therefore simplistic approaches to represent the chemistry are used. Here we examine the variability between different chemistry schemes. To achieve this, we employ a state-of-the-art Earth System Model to compare seven simulations with differing sulfur-related chemical reactions. We show that sulfate chemistry contributes to large uncertainties in aerosol and cloud formation. This work underscores the need to improve sulfur chemistry to improve the accuracy of cloud and aerosol projections in a warming world.

## 1 Introduction

Dimethyl sulfide (DMS;  $\text{CH}_3\text{SCH}_3$ ) is the primary natural source of atmospheric sulfur-containing species (Breider et al., 2010; Boucher et al., 2003). DMS is produced from the biogeochemical activity of marine biota (Charlson et al., 1987; Keller et al., 1989; Bates et al., 1987), and when emitted into the atmosphere, undergoes numerous chemical reactions, some of which lead to the formation of sulfate aerosols (Hoffmann et al., 2021; Chen et al., 2018). Aerosols play an important role in cloud formation and influence Earth’s energy balance (Carslaw et al., 2013; Novak et al., 2021).

Both natural (biogenic) and anthropogenic emissions contribute to the global sulfur cycle. In the Northern Hemisphere (NH), atmospheric sulfur originates primarily from anthropogenic sources such as power stations and ship emissions (e.g. Smith et al., 2011). In contrast, natural sources dominate atmospheric sulfur loading in the Southern Hemisphere (SH), with anthropogenic sources contributing only 30% – 50% (Kloster et al., 2006; Korhonen et al., 2008). Emissions of anthropogenic sulfur-containing gases are well-represented in climate models (Hoesly et al., 2018; Hardacre et al., 2021; Turnock et al., 2020). In contrast, there are significant uncertainties regarding natural sulfur emissions, especially over the remote Southern Ocean where DMS emissions are large and observations are sparse (Bhatti et al., 2023; Bock et al., 2021; Hulswar et al., 2022).

The Southern Ocean region has a vital role in the global sulfur cycle but is predominantly of natural origin, which is one of the largest sources of uncertainty for the sulfur cycle (Hoesly et al., 2018; Fung et al., 2022). This region is where global DMS production maximizes but is poorly constrained in models (Belviso et al., 2004; Bock et al., 2021; Revell et al., 2019), and is closely examined in this work.

Previously we examined the sensitivity of atmospheric DMS to oceanic DMS concentrations and sea-to-atmosphere transfer velocities in a global climate model (Bhatti et al., 2023). Here, we examine the sensitivity of sulfate aerosol formation to the model’s DMS and sulfate chemistry scheme. Whilst there is active work in the improvement of DMS mechanisms used for modelling (e.g. Cala et al., 2023), current generation climate models use relatively similar DMS and sulfate chemistry schemes, but with slight differences (e.g. Archibald et al., 2020; Horowitz et al., 2020; Sheng et al., 2015). We implemented seven such chemistry schemes taken from other climate models into a single model, and assessed uncertainties in aerosol and cloud properties associated with sulfate chemistry. Model configurations and simulation descriptions are described in Section 2, and results are shown in Section 3.

## 2 Methods

### 2.1 Model Configuration and Simulations Performed

Simulations were performed with the atmosphere-only configuration of the UK Earth System Model (UKESM1-AMIP), which operates on a grid with a resolution of  $1.25^\circ$  latitude  $\times$   $1.85^\circ$  longitude (Sellar et al., 2019). All simulations were performed with an oceanic DMS data set calculated from satellite chlorophyll *a* observations, which is described and evaluated by Bhatti et al. (2023). DMS emissions are calculated using the transfer velocity from Blomquist et al. (2017). Atmospheric oxidation of DMS is handled via the StratTrop chemistry scheme (labelled here as ‘REF’; Archibald et al., 2020; Mulcahy et al., 2020), which is modified for the sensitivity simulations.

Aerosol microphysics is determined using the Global Model of Aerosol Processes (GLOMAP-mode) – a two-moment modal aerosol microphysics scheme. This scheme simulates various aerosol species across five lognormal size modes: nucleation mode, soluble Aitken mode, accumulation mode, coarse mode, and insoluble Aitken mode (Mulcahy et al., 2020). Typically, aerosols with a radius of  $\geq 25$  nm (Aitken mode) are activated into cloud condensation nuclei (CCN) and cloud droplets (Walters et al., 2019; Abdul-Razzak & Ghan, 2000). A constant cloud water pH of 5.0 is used in the UKESM1, which is important for aqueous-phase chemistry (Turnock et al., 2019). Greenhouse gas concentrations and anthropogenic aerosol emissions follow Coupled Model Intercomparison Project phase 6 (CMIP6) recommendations.

Simulations were run for three years, from January 2016 to December 2018, with the first year discarded as spin-up. Wind and temperature are nudged to values from the ERA-5 reanalysis at 6-hourly intervals (Hersbach et al., 2020; Dee et al., 2011).

Six sensitivity simulations were performed using DMS and sulfate chemistry schemes from other Earth system models, many of which participated in CMIP6 (Table 1). For detailed DMS and non-DMS sulfur reactions, refer to Tables S1 and S2. In terms of gas-phase chemistry, all schemes feature an OH addition and abstraction pathway. All schemes also include a  $\text{NO}_3$  oxidation reaction for DMS, except MIROC. None include the newly-identified hydroperoxymethyl thioformate, a DMS oxidation product (HPMTF; Veres et al., 2020), although its role is actively researched (Cala et al., 2023; Fung et al., 2022). All schemes involve at least two aqueous-phase in-cloud reactions. StratTrop, CHEM3, and GEOS-CHEM have a third aqueous-phase reaction with  $\text{O}_3$ . CHEM3 and GEOS-CHEM have the largest number of aqueous-phase reactions (Revell et al., 2019; Chen et al., 2017, 2016). Methanesulfonic acid (MSA), which is produced by DMS reacting with OH, is treated as a sink for DMS in UKESM1-AMIP and is not transported or advected (Mulcahy et al., 2020). Differences between each model tuning mean that the spread between chemistry schemes will be smaller if doing an intercomparison using their own model. Here we go further than just testing expansions of sulfate chemistry schemes, but

quantifying how much variability in DMS and aerosol can result just from using CMIP6 or well-established chemistry schemes.

We quantify the spread between the simulations in the values derived from the various chemistry schemes using the relative range in percentage. This is calculated by the difference between the largest and smallest values, divided by the smallest value, and then multiplied by 100.

**Table 1.** Chemical reactions used in each simulation. Light gray shading: DMS oxidation reactions. Medium gray shading: gas-phase reactions involving DMS oxidation products. Dark gray shading: aqueous phase reactions involving sulfur-containing species. All reactions are gas-phase unless otherwise indicated. All models contain two DMS + OH reactions; abstraction and addition. For reaction rates and references see Tables S1 and S2.

Chemical Reaction	REF	SEN-SOCOL <sup>a</sup>	SEN-MIROC <sup>b</sup>	SEN-GFDL <sup>c</sup>	SEN-GEOS-CHEM <sup>d</sup>	SEN-CHEM3	SEN-NorESM <sup>e</sup>
DMS + OH (abs)							
DMS + OH (add)							
DMS + NO <sub>3</sub>							
DMS + ClO							
DMS + Br							
DMS + BrO							
DMS + O <sub>3</sub>							
DMS + Cl							
DMS( <i>aq</i> ) + O <sub>3</sub> ( <i>aq</i> )							
SO <sub>2</sub> + OH							
SO <sub>2</sub> + O							
SO <sub>2</sub> + O <sub>3</sub>							
SO <sub>3</sub> + H <sub>2</sub> O							
DMSO + OH							
MSIA + O <sub>3</sub>							
MSIA + OH							
S(IV) + H <sub>2</sub> O <sub>2</sub> ( <i>aq</i> )							
S(IV) + O <sub>3</sub> ( <i>aq</i> )							
S(IV) + O <sub>3</sub> ( <i>aq</i> )							
S(IV) + HOBr( <i>aq</i> )							
S(IV) + HOBr( <i>aq</i> )							
O <sub>3</sub> ( <i>aq</i> ) + MSI <sup>-c</sup> <sub>(aq)</sub>							
O <sub>3</sub> ( <i>aq</i> ) + MSIA( <i>aq</i> )							
S(IV) + HO <sub>2</sub> NO <sub>2</sub> ( <i>aq</i> )							

<sup>a</sup> Solar-climate Ozone Links (SOCOL)

<sup>b</sup> Model for Interdisciplinary Research on Climate (MIROC)

<sup>c</sup> Geophysical Fluid Dynamics Laboratory (GFDL)

<sup>d</sup> Goddard Earth Observing System (GEOS)

<sup>e</sup> Norwegian Earth System Model (NorESM)

## 2.2 Observational Data Sets

Satellite, ground, and ship-based observations were used for model evaluation (Table S3). Data from the Southern Ocean, representing a region largely untouched by anthropogenic aerosol emissions, are limited. To evaluate atmospheric DMS in this region we merge ground and ship-based data into one data set, each weighted equally across each month. Only two sources offer DMS data for the Austral winter, but the summer and autumn are represented by seven datasets (Table S3).

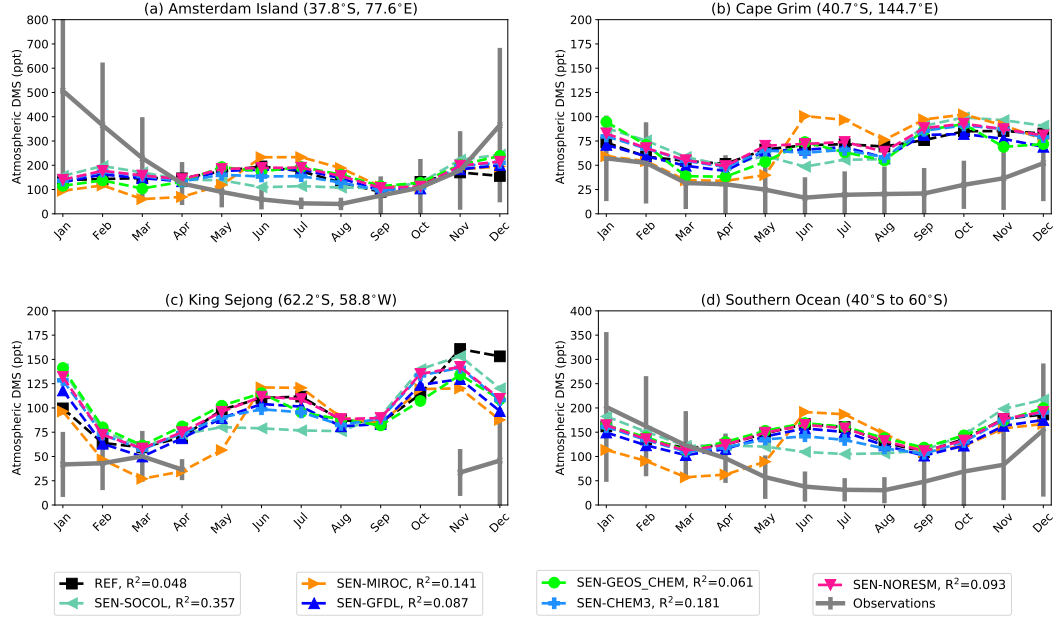


**Figure 1.** Southern Ocean atmospheric DMS surface concentrations showing climatological monthly-means for the simulations comparing differing sulfate chemistry schemes with observations. Lines show the observational means (in grey) and their standard deviation (error bars) compared with the simulations for the same grid cells. The Southern Ocean measurements are compiled from 3 ground-based stations and 4 voyages, all weighted equally. The average  $R^2$  value represents the seasonal correlation coefficient between the simulation and each respective observation.

### 3 Results and Discussion

The Southern Ocean (40 °S to 60 °S) is a focus of this study to investigate the different sulfate chemistry schemes used in the model simulations, and to compare with observations of atmospheric DMS. This region’s global importance for DMS is highlighted by the high proportion of atmospheric DMS from the Southern Ocean contributing towards the global atmospheric DMS burden with 49% to 70% shown by our simulations.

Average DMS concentrations are relatively well constrained between the simulations, which is unsurprising given that all simulations used the same oceanic DMS source and sea-to-air transfer velocity. Previous work has evaluated DMS and other aerosol properties in UKESM1-AMIP (Bhatti et al., 2023; Mulcahy et al., 2020). Bhatti et al. (2023) identified a 171% spread in DJF atmospheric DMS from Southern Ocean DMS concentrations and emissions, whereas the spread identified from the simulations performed here during the same period and region is 48%. Although the emissions and concentrations drive much of the spatial and seasonal variability of atmospheric DMS, we demonstrate that differences in CMIP6 chemistry also have a profound influence on Southern Ocean atmospheric DMS. Here we examine the seasonal cycle in DMS from available observations (Figure 1).

As shown in Figure 1, all simulations overestimate austral wintertime (JJA) atmospheric DMS but generally are closer to observations in summer months, except at Amsterdam Island. The year-long observational stations display a clear seasonal cycle for Southern Ocean DMS; however, none of the simulations successfully capture the DMS depletion during winter. The SOCOL chemistry scheme enables UKESM1-AMIP to best

represent the seasonal cycle in atmospheric DMS ( $R^2 = 0.357$  compared to observations;  $R^2 < 0.2$  for all other simulations).

The current representation of the UKESM1-AMIP Southern Ocean DMS may be flawed during the wintertime, as demonstrated by increases in DMS concentrations which are not observed in any observations (Figure 1). DMS is mostly oxidized via  $\text{NO}_3$  during austral winter, however, most simulations do not oxidize DMS quickly enough, resulting in an accumulation of DMS during winter from the less efficient wintertime loss pathway, which SEN-SOCOL shows. The additional Cl and Br chemistry is therefore an important source for DMS oxidation during winter, in agreement with Chen et al. (2018). Although the distribution of atmospheric DMS is mostly controlled by the oceanic DMS and DMS emissions (Bhatti et al., 2023), we demonstrate the importance of choosing a sulfate chemical reaction scheme appropriately over the Southern Ocean. As a result, we investigate the global differences in chemical oxidation of DMS between each simulation.

### 3.1 Chemical oxidation of DMS

Globally, DMS + OH reactions account for 56% to 65% of total DMS loss in our simulations (Figure 2), in agreement with Fung et al. (2022). DMS oxidation via the OH addition and abstraction pathways dominates other oxidation reactions in the Southern Hemisphere, while DMS +  $\text{NO}_3$  is largest in the Northern Hemisphere where there are large anthropogenic nitrate emissions. The hemispheric distribution of the widely used DMS reactions (DMS + OH and DMS +  $\text{NO}_3$ ) is consistent with Chen et al. (2018).

Global DMS lifetimes of 1.2 to 1.4 days are consistent with the literature estimates of 0.72 to 2.34 days (Breider et al., 2010; Mulcahy et al., 2020). Figure S1 shows the spatial distribution of DMS lifetimes for each simulation. SEN-SOCOL (Figures 2b and S1b) has more DMS oxidized by  $\text{NO}_3$  at the high SH latitudes than the other chemistry schemes, therefore reducing the lifetime of DMS, especially during winter. This reduces the relative importance of DMS oxidation via OH.

In SEN-GEOS-CHEM, there is more DMS oxidation by  $\text{NO}_3$  over continental regions than in the other simulations due to the high availability of  $\text{NO}_3$  (Figures 2e and S1e). Reducing the reaction rate constant for DMS oxidation with  $\text{NO}_3$  tends to extend the DMS lifetime for the simulations, particularly during the night when  $\text{NO}_3$  is often the only DMS loss pathway for many chemistry schemes. SEN-MIROC, without a DMS +  $\text{NO}_3$  reaction, lengthens the DMS lifetime over high northern latitudes (Figure S1), in contrast to the other simulations. However, SEN-MIROC contains an alternative DMS loss pathway via DMSO, and essentially becomes a night loss mechanism for DMS (not shown), compensating for the lack of DMS +  $\text{NO}_3$  reaction.

The inclusion of additional DMS oxidation pathways (e.g. ozone, reactive chlorine, and bromine) as in SOCOL and CHEM3 has a relatively minor impact on DMS oxidation. UKESM1-AMIP currently only has a stratospheric source of inorganic chlorine or bromine, which explains why the contribution of these pathways is close to zero in Figure 2b,f. Future work will investigate the impacts on sulfur chemistry by implementing tropospheric inorganic chlorine and bromine sources.

Of all the chemistry schemes used here, only SEN-GFDL has up-to-date rate constant parameters for DMS oxidation as recommended by the latest JPL report (Table S1; Burkholder et al. (2020)). Our results show some, but minor differences in DMS lifetime and concentrations when comparing simulations with up-to-date rate constants to those without (Figures 2 and 1). We therefore suggest that other modeling groups regularly ensure rate constant parameters are up-to-date to have more accurate DMS reactions. Expanding the analysis to other sulfur species, including DMS, which are instrumental towards aerosol formation is further evaluated below.

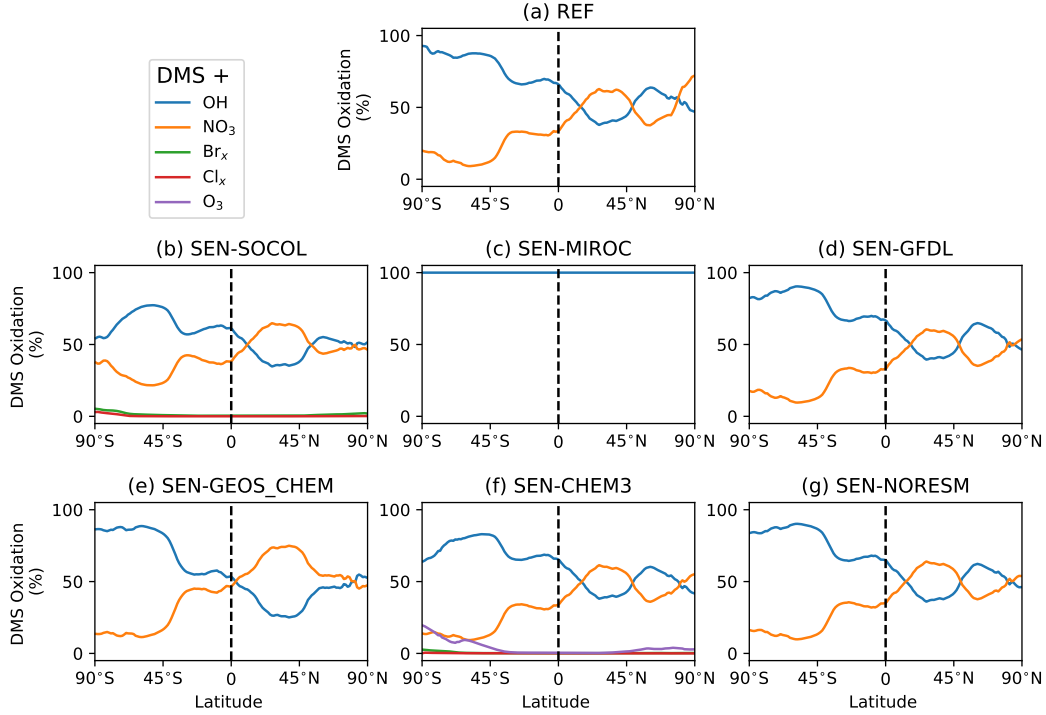


**Figure 2.** Zonal annual means of the relative proportions of all chemical reactions (%) involved in DMS oxidation. The sum of all reactions for each simulation equals 100%. The dashed line indicates the equator.  $\text{Br}_x = \text{Br}$  and/or  $\text{BrO}$  and  $\text{Cl}_x = \text{Cl}$  or  $\text{ClO}$ . See Table 1 for more details.

### 3.2 Aerosol Response to Sulfate Chemistry Schemes

To better understand the differences in aerosol between the simulations with differing sulfate chemistry, we examine differences in the aerosol modes and CCN and  $\text{H}_2\text{SO}_4$  concentrations. Number concentrations of aerosol in different modes from our simulations are shown in Figure 3 (a-c for NH, g-i for SH). We exclude coarse mode aerosols which are dominated by sea spray in UKESM1-AMIP.

The nucleation mode over both hemispheres has a much higher sensitivity to changes in the chemistry scheme than the other modes, from the higher number of nucleation mode particles from anthropogenic sulfur sources. Simulations over the NH have an aerosol number concentration around three times higher than the SH with the NH having 129% more nucleating particles (Figures 3a, g and 3f, l). Similarly,  $\text{H}_2\text{SO}_4$  has much higher concentrations over the NH (Figures 3d,j). This is due to a much higher anthropogenic contribution.

In both the NH and SH SEN-NorESM has lower Aitken and accumulation mode concentrations compared to most of the other simulations which leads to lower AOD and CCN. This can be attributed to the scheme using only one  $\text{SO}_2$  oxidation pathway, reducing atmospheric sulfate available for conversion to aerosol. As aerosols grow from the nucleation mode, they have a greater influence on cloud formation (Figure 3e, k). SEN-GEOS-CHEM and SEN-CHEM3 have the highest CCN concentrations due to a larger number of in-cloud reactions which enhances aerosol growth into the accumulation mode. Simulations with more aqueous-phase chemistry may allow more sulfate aerosol to transfer into larger aerosol modes. For example, shown in Figure 3a, the SEN-GEOS-CHEM



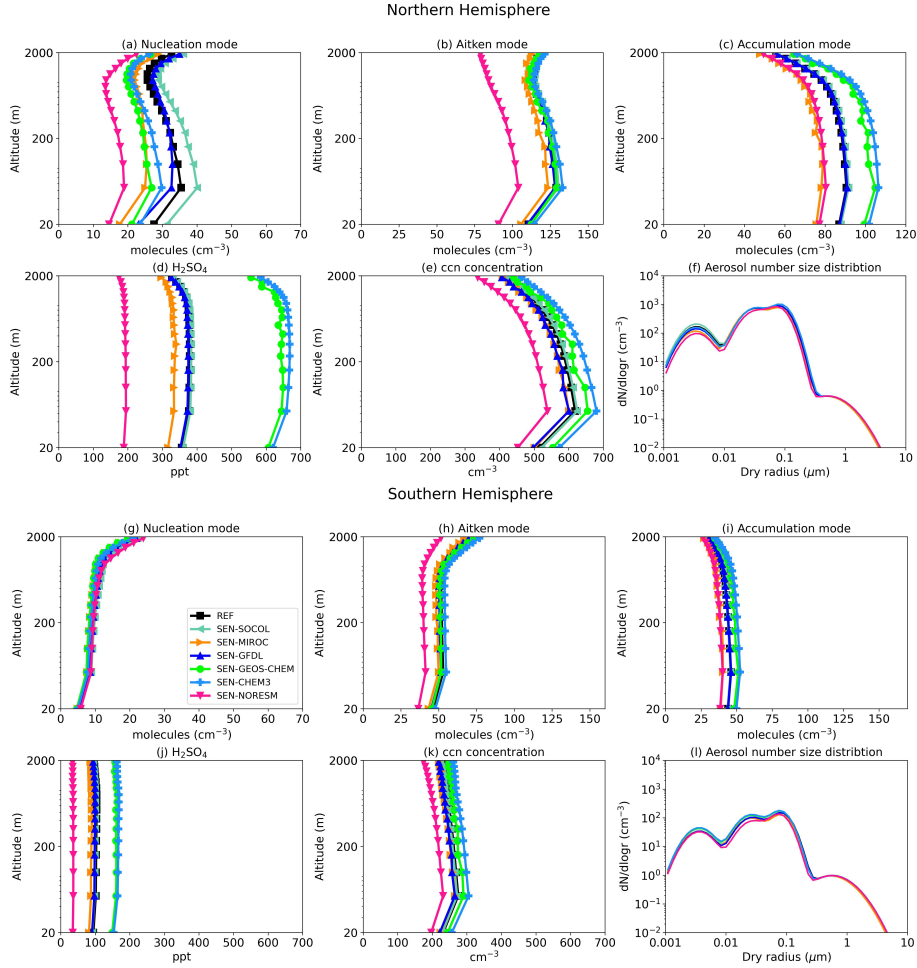


**Figure 3.** Global averaged aerosol number concentrations from the (a,g) nucleation-mode, (b,h) Aitken-mode, (c,i) accumulation-mode. (d,j) The  $\text{H}_2\text{SO}_4$  abundance is shown in parts per trillion (ppt). (e,k) Cloud condensation nuclei and (f,l) Global aerosol number size distributions are also shown. (a - f): Northern Hemisphere average; (g - l): Southern Hemisphere average.

and SEN-CHEM3 simulations contain fewer nucleation mode aerosol concentrations than the REF simulation. However, SEN-GEOS-CHEM and SEN-CHEM3 contain the highest concentrations within the larger modes (Figure 3c,i).

Accurately representing cloud-water pH in climate models is crucial for aqueous-phase chemistry and cloud formation (Turnock et al., 2019). Global cloud water pH varies between 3-8, however, UKESM1 uses a uniform value of 5 (Shah et al., 2020). A small increase in pH could reduce the number of aerosols serving as CCN (Turnock et al., 2019). Chemistry schemes used in their native models are effectively tailored to that models specific configurations. For example, GEOS-CHEM has interactive cloud-water pH affecting aerosol modes differently to the UKESM1 (Alexander et al., 2012). Other models, like GFDL, assume cloud water pH of 4.5, leading to differences in their aqueous-phase reactions (Krasting et al., 2018; Turnock et al., 2016). DMS oxidation into  $\text{SO}_4^{2-}$  can also impact pH (Shah et al., 2020), particularly in DMS-rich areas like the Southern Ocean. Excessive oxidation can lower the pH, impacting cloud formation. Thus, assuming a uni-



form cloud-water pH for the Southern Ocean will lead to model spread, given the significant oxidation variations across simulations. Further work in updating the UKESM1 chemistry sources is therefore needed to better represent aerosols and DMS. For instance, the inclusion of a BrO inorganic source from sea-spray would provide a much greater avenue for DMS oxidation during the winter, which has been shown to have a substantial impact (Breider et al., 2010; Fung et al., 2022).

### 3.3 Sensitivity to Sulfate Chemistry Schemes

To assess the overall sensitivity of sulfate formation to atmospheric chemistry, we analyze simulated DMS, AOD, cloud droplet number concentration (CDNC), and all-sky shortwave radiation at the top of the atmosphere relative to the  $\text{SO}_4$  mass fraction (which is integrated between the surface and top-of-atmosphere; Figure 4).

The spread between all the simulations annual mean is 20% for DMS globally. The DMS burden is reasonably well constrained (ranging between 35-44 Gg S globally; (Figure 4a). The vertical error bars are larger in the SH than in the NH because of the large seasonality in marine biogenic activity at southern high latitudes (Figure 4e, i; Jarníková & Tortell (2016); Curran & Jones (2000)). With the exception of the MIROC scheme, the spread is 12% in DMS burden across the models. The MIROC chemistry scheme omits the  $\text{DMS} + \text{NO}_3$  oxidation reaction, which is important in the removal of DMS over the NH due to anthropogenic nitrate emissions (Archer-Nicholls et al., 2023; Chen et al., 2018).

The global contribution of atmospheric DMS to the overall sulfur burden ( $\text{DMS}_{\text{sulfur}}$ ) across all simulations, varies between 13.6% to 25.4% (Table S4). Four simulations (SEN-SOCOL, REF, SEN-GFDL, SEN-CHEM3) have the lowest  $\text{DMS}_{\text{sulfur}}$ , shown in Figure 4a and Tables S4 and S5. Although SEN-NorESM has the lowest sulfur burden, it has the highest proportion of sulfur from DMS (Table S4). Existing estimates of global  $\text{DMS}_{\text{sulfur}}$  are between 10% to 32% (Gondwe et al., 2003; Kloster et al., 2006; Fung et al., 2022). SEN-MIROC has almost double the average DMS burden over the NH likely due to the lack of  $\text{NO}_3$  reactions with DMS as discussed above. Around 80% of the global annual average  $\text{DMS}_{\text{sulfur}}$  is sourced entirely from SH annual average DMS (Table S4).

Figure 4a,e,i demonstrates that simulations with very similar DMS burdens have very different  $\text{SO}_4$  burdens driven by the different sulfate mechanisms/oxidation pathways. The spread in the global annual mean  $\text{SO}_4$  mass fraction across the simulations is 308%.  $\text{SO}_4$  is crucial for the formation of clouds and aerosol (Figure 4) and consequently global annual mean AOD and CDNC have a spread of 79% (0.077) and 70% ( $44 \text{ cm}^{-3}$ ) across our simulations (Figure 4b,c). The spread in AOD between our simulations is much greater than the AOD of 0.031 from CMIP6 models (Vogel et al., 2022). Additionally, global annual mean AOD is suggested to have only increased by 0.04 to 0.046 since pre-industrial times, with CDNC also increasing by 10 to  $20 \text{ cm}^{-3}$ , highlighting the large variation between the chemistry schemes (Seo et al., 2020; Tsigaridis et al., 2006; Bhatti et al., 2022; Bauer et al., 2020; Kirkevåg et al., 2018). The spread of the simulations between both hemispheres is the same for CDNC but is two times greater over the NH than the SH for AOD. For all simulations, there is a linear relationship between AOD and CDNC vs  $\text{SO}_4$  mass fraction: the chemistry schemes that oxidize DMS and sulfate more efficiently (such as SEN-GEOS-CHEM and SEN-CHEM3) also produce more AOD and CDNC. All simulations showing AOD and CDNC over the SH are closer to the observed AOD and CDNC averages. Future work will quantify what fraction of the spread in aerosol is driven by DMS and from anthropogenic sulfur.

SEN-NorESM has the lowest AOD, CDNC, and  $\text{SO}_4$  mass fraction, but an average DMS burden. This is likely due to inefficient sulfur-to-aerosol conversion over the NH demonstrated by a higher sulfur burden and fewer reactions involving  $\text{SO}_4$  products than other schemes (Table S2). More specifically, the lower aerosol likely results from

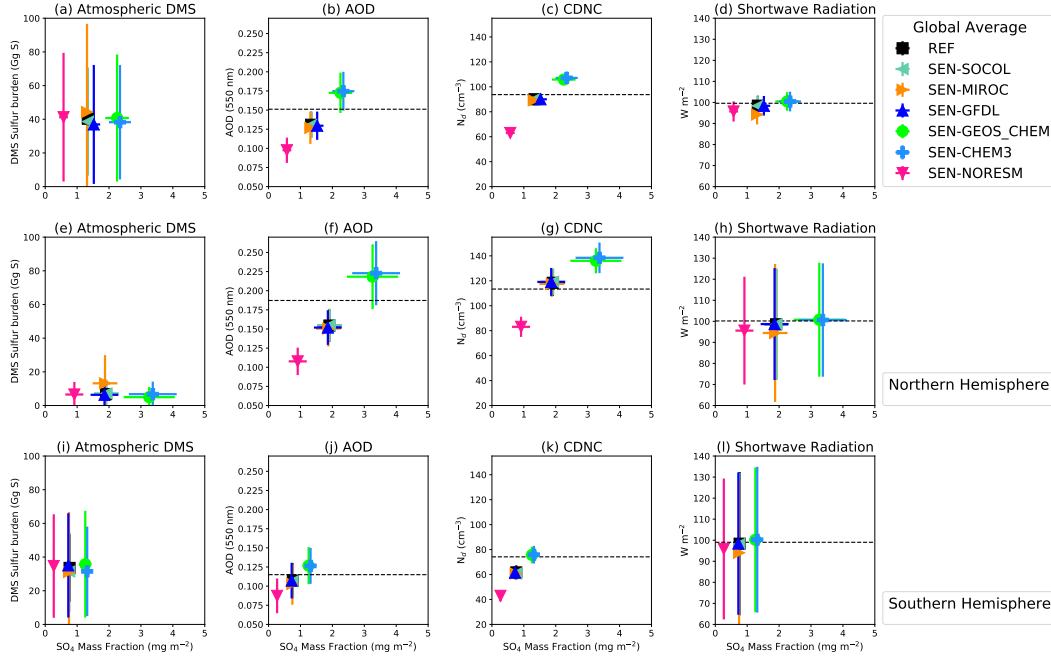


**Figure 4.** Annual-mean atmospheric DMS sulfur burden, AOD, CDNC, and shortwave radiation as a function of the vertically integrated  $\text{SO}_4$  mass fraction. Top row: global average; middle row: Northern Hemisphere; bottom row: Southern Hemisphere. The dashed horizontal line represents the average value from observations. First column: atmospheric DMS (no global observations are available); second column: MODIS AOD (Platnick et al., 2017); third column: CDNC satellite measurements at cloud top between 2017 to 2018 from Grosvenor et al. (2018); fourth column: TOA all-sky shortwave radiation from CERES (Loeb et al., 2018). Error bars show the standard deviation on spatially averaged quantities calculated over the two-year simulations.

decreased  $\text{SO}_4$  mass fraction (Figure 4) and less efficient  $\text{SO}_2$  oxidation into  $\text{H}_2\text{SO}_4$ , as discussed in Section 3.2.

The CHEM3 scheme is a modified version of the SEN-GEOS-CHEM DMS and sulfate chemistry scheme, with both simulations simulating the largest global CDNC (Chen et al., 2018; Revell et al., 2019). Revell et al. (2019) showed that SEN-CHEM3 leads to increased CDNC over the Southern Ocean due to the inclusion of additional aqueous-phase sulfate reactions. Despite pronounced differences in global mean CDNC ( $63\text{--}107\text{ cm}^{-3}$ , Figure 4c), differences in top-of-atmosphere all-sky shortwave radiation are relatively small between the simulations (Figure 4d,h,l).

## 4 Summary and Conclusions

This study compares the differences between sulfate chemistry schemes using identical base configurations. The sensitivity of DMS and its oxidation products to changes in sulfate chemistry was investigated using a nudged configuration of the UKESM1-AMIP model. We show that testing 7 sulfate chemistry schemes in one model causes large variations in  $\text{SO}_4$ , CDNC, and AOD across simulations; twice the change in AOD and CDNC between the pre-industrial and the present-day when simulated in UKESM1 (Seo et al., 2020; Bauer et al., 2020). Additional aqueous-phase chemistry increases the inter-model

variance through an increased number of larger aerosols. Our results need further investigation to determine if they would be universally robust. For example, because of differences in model formulation (grid box sizes, oxidant levels and many other processes), we don't expect the same sensitivities we have calculated here across other "base models" – and we encourage work that would address this issue as a priority. As each model treats DMS and sulfur chemistry and aerosol microphysical processes differently from UKESM1, such as differences in cloud water pH or aerosol size distributions, the spread in AOD (0.077) is more than double that compared between CMIP6 simulations (0.031; Vogel et al. (2022)). Therefore, careful consideration is necessary when modifying sulfate chemistry schemes in climate models as aerosol response may vary significantly. We highlight the associated uncertainty to aerosol and CDNC from sulfate chemistry seems to be significantly large enough that it may alter the pre-industrial baseline and therefore be an important source of uncertainty in aerosol ERF estimates. Therefore our study builds on previous perturbed parameter ensemble studies of aerosol parameters which did not consider these parameters (Carslaw et al., 2013)

We demonstrate that differences between well-established DMS and sulfate aerosol chemistry schemes can strongly impact the global spread of DMS concentrations by as much as 20% between the simulations, with larger fluctuations over the NH. These global differences arise from differences in DMS oxidation pathways. Large seasonal differences are also present between the simulations over the Southern Ocean, with the closest simulation to observations coming from the SOCOL chemistry scheme ( $R^2$  of 0.36). The UKESM1-AMIP currently lacks an inorganic BrO source from sea-spray which may provide improvements to comparisons with observations, especially during the winter. The spread in Southern Ocean DJF atmospheric DMS associated with chemistry (48%) is less than the spread from oceanic concentration and emissions (171%).

This work demonstrates the importance of DMS and sulfate chemistry in future model intercomparison projects for future aerosol modeling. Overall, we find that testing different sulfate chemistry schemes in a single model can strongly affect aerosols and cloud formation.

## 5 Open Research

The MODIS-aqua satellite data from AOD and chlorophyll *a* are available in <https://giovanni.gsfc.nasa.gov/giovanni/>. CDNC observational data are available from <https://doi.org/10.5285/864a46cc65054008857ee5bb772a2a2b>. The CERES data was obtained in <https://ceres.larc.nasa.gov/data/>. DMS measurements are available at <https://ebas-data.nilu.no/Default.aspx>. Model simulation data are archived at New Zealand eScience Infrastructure (NeSI; <https://www.nesi.org.nz/>). As all simulation data is over 1 Terabyte, they will be managed and made available for at least 5 years by contacting the corresponding author.

## Acknowledgments

This research was supported by the Deep South National Science Challenge (Grant Numbers C01X141E2 and C01X1901). We acknowledge the UK Met Office for the use of the UM. We also acknowledge the contribution of NeSI high-performance computing facilities to the results of this research. New Zealand's national facilities are provided by NeSI and funded jointly by NeSI's collaborator institutions and through the Ministry of Business, Innovation and Employment's Research Infrastructure programme (<https://www.nesi.org.nz/>). We acknowledge the Cape Grim Science Program for the provision of DMS data from Cape Grim. The Cape Grim Science Program is a collaboration between the Australian Bureau of Meteorology and the CSIRO Australia. LER appreciates support by the Rutherford Discovery Fellowships from New Zealand Government funding, administered by the Royal Society Te Apārangi.

## References

- Abdul-Razzak, H., & Ghan, S. J. (2000). A parameterization of aerosol activation: 2. Multiple aerosol types. *Journal of Geophysical Research: Atmospheres*, 105(D5), 6837–6844. doi: 10.1029/1999JD901161
- Alexander, B., Allman, D. J., Amos, H. M., Fairlie, T. D., Dachs, J., Hegg, D. A., & Sletten, R. S. (2012). Isotopic constraints on the formation pathways of sulfate aerosol in the marine boundary layer of the subtropical northeast Atlantic Ocean. *Journal of Geophysical Research: Atmospheres*, 117(D6). doi: <https://doi.org/10.1029/2011JD016773>
- Archer-Nicholls, S., Allen, R., Abraham, N. L., Griffiths, P. T., & Archibald, A. T. (2023, May). Large simulated future changes in the nitrate radical under the CMIP6 SSP scenarios: implications for oxidation chemistry. *Atmospheric Chemistry and Physics*, 23(10), 5801–5813. (Publisher: Copernicus GmbH) doi: 10.5194/acp-23-5801-2023
- Archibald, A. T., O'Connor, F. M., Abraham, N. L., Archer-Nicholls, S., Chipperfield, M. P., Dalvi, M., ... Zeng, G. (2020). Description and evaluation of the UKCA stratosphere–troposphere chemistry scheme (StratTrop vn 1.0) implemented in UKESM1. *Geoscientific Model Development*, 13(3), 1223–1266. doi: 10.5194/gmd-13-1223-2020
- Bates, T. S., Cline, J. D., Gammon, R. H., & Kelly-Hansen, S. R. (1987). Regional and seasonal variations in the flux of oceanic dimethylsulfide to the atmosphere. *Journal of Geophysical Research: Oceans*, 92(C3), 2930–2938. (Publisher: Wiley Online Library)
- Bauer, S. E., Tsigaridis, K., Faluvegi, G., Kelley, M., Lo, K. K., Miller, R. L., ... Wu, J. (2020). Historical (1850–2014) Aerosol Evolution and Role on Climate Forcing Using the GISS ModelE2.1 Contribution to CMIP6. *Journal of Advances in Modeling Earth Systems*, 12(8), e2019MS001978. doi: 10.1029/2019MS001978
- Belviso, S., Bopp, L., Moulin, C., Orr, J. C., Anderson, T., Aumont, O., ... Simó, R. (2004, September). Comparison of global climatological maps of sea surface dimethyl sulfide. *Global Biogeochemical Cycles*, 18(3). (Publisher: American Geophysical Union) doi: 10.1029/2003GB002193
- Bhatti, Y., Cozzi, L., & McDonald, A. (2022). Influences of Antarctic ozone depletion on Southern Ocean aerosols. *Journal of Geophysical Research: Atmospheres*, 127(18), e2022JD037199. (Publisher: Wiley Online Library) doi: <https://doi.org/10.1029/2022JD037199>
- Bhatti, Y., Revell, L., Schuddeboom, A., McDonald, A., Archibald, A., Williams, J., ... Behrens, E. (2023, May). *The sensitivity of Southern Ocean atmospheric dimethyl sulfide to modelled sources and emissions* (preprint). doi: 10.5194/egusphere-2023-868
- Blomquist, B. W., Brumer, S. E., Fairall, C. W., Huebert, B. J., Zappa, C. J., Brooks, I. M., ... others (2017). Wind speed and sea state dependencies of air-sea gas transfer: Results from the High Wind speed Gas exchange Study (HiWinGS). *Journal of Geophysical Research: Oceans*, 122(10), 8034–8062. (Publisher: Wiley Online Library)
- Bock, J., Michou, M., Nabat, P., Abe, M., Mulcahy, J. P., Olivié, D. J., ... others (2021). Evaluation of ocean dimethylsulfide concentration and emission in CMIP6 models. *Biogeosciences*, 18(12), 3823–3860. (Publisher: Copernicus GmbH)
- Boucher, O., Moulin, C., Belviso, S., Aumont, O., Bopp, L., Cosme, E., ... Venkataraman, C. (2003). DMS atmospheric concentrations and sulphate aerosol indirect radiative forcing: a sensitivity study to the DMS source representation and oxidation. *Atmospheric Chemistry and Physics*, 3(1), 49–65. (Publisher: Copernicus GmbH) doi: 10.5194/acp-3-49-2003
- Breider, T. J., Chipperfield, M. P., Richards, N. a. D., Carslaw, K. S., Mann,

- 409 G. W., & Spracklen, D. V. (2010). Impact of BrO on dimethylsulfide in the  
 410 remote marine boundary layer. *Geophysical Research Letters*, *37*(2). doi:  
 411 10.1029/2009GL040868
- 412 Burkholder, J., Sander, S., Abbatt, J., Barker, J., Cappa, C., Crounse, J., ...  
 413 Kurylo, M. (2020). *Chemical kinetics and photochemical data for use in atmo-*  
 414 *spheric studies; evaluation number 19* (Report). Pasadena, CA: Jet Propulsion  
 415 Laboratory, National Aeronautics and Space ...
- 416 Cala, B. A., Archer-Nicholls, S., Weber, J., Abraham, N. L., Griffiths, P. T., Jacob,  
 417 L., ... Archibald, A. T. (2023). Development, intercomparison and evaluation of  
 418 an improved mechanism for the oxidation of dimethyl sulfide in the UKCA model.  
 419 *Atmospheric Chemistry and Physics*, 1–51. (Publisher: Copernicus GmbH)
- 420 Carslaw, K. S., Lee, L. A., Reddington, C. L., Pringle, K. J., Rap, A., Forster,  
 421 P. M., ... Pierce, J. R. (2013). Large contribution of natural aerosols to uncer-  
 422 tainty in indirect forcing. *Nature*, *503*(7474), 67–71. doi: 10.1038/nature12674
- 423 Charlson, R. J., Lovelock, J. E., Andreae, M. O., & Warren, S. G. (1987).  
 424 Oceanic phytoplankton, atmospheric sulphur, cloud albedo and climate. *Nature*,  
 425 *326*(6114), 655–661.
- 426 Chen, Q., Geng, L., Schmidt, J. A., Xie, Z., Kang, H., Dachs, J., ... Alexander,  
 427 B. (2016, September). Isotopic constraints on the role of hypohalous acids in  
 428 sulfate aerosol formation in the remote marine boundary layer. *Atmospheric*  
 429 *Chemistry and Physics*, *16*(17), 11433–11450. (Publisher: Copernicus GmbH) doi:  
 430 10.5194/acp-16-11433-2016
- 431 Chen, Q., Schmidt, J. A., Shah, V., Jaeglé, L., Sherwen, T., & Alexander, B. (2017).  
 432 Sulfate production by reactive bromine: Implications for the global sulfur and  
 433 reactive bromine budgets. *Geophysical Research Letters*, *44*(13), 7069–7078. doi:  
 434 10.1002/2017GL073812
- 435 Chen, Q., Sherwen, T., Evans, M., & Alexander, B. (2018). DMS oxidation and sul-  
 436 fur aerosol formation in the marine troposphere: a focus on reactive halogen and  
 437 multiphase chemistry. *Atmospheric Chemistry and Physics*, *18*(18), 13617–13637.  
 438 doi: 10.5194/acp-18-13617-2018
- 439 Curran, M. A., & Jones, G. B. (2000). Dimethyl sulfide in the Southern Ocean:  
 440 Seasonality and flux. *Journal of Geophysical Research: Atmospheres*, *105*(D16),  
 441 20451–20459. (Publisher: Wiley Online Library)
- 442 Dee, D. P., Uppala, S. M., Simmons, A. J., Berrisford, P., Poli, P., Kobayashi, S., ...  
 443 Vitart, F. (2011). The ERA-Interim reanalysis: configuration and performance  
 444 of the data assimilation system. *Quarterly Journal of the Royal Meteorological*  
 445 *Society*, *137*(656), 553–597. doi: 10.1002/qj.828
- 446 Fung, K. M., Heald, C. L., Kroll, J. H., Wang, S., Jo, D. S., Gettelman, A., ...  
 447 Zawadowicz, M. (2022). Exploring dimethyl sulfide (DMS) oxidation and impli-  
 448 cations for global aerosol radiative forcing. *Atmospheric Chemistry and Physics*,  
 449 *22*(2), 1549–1573. (Publisher: Copernicus GmbH) doi: 10.5194/acp-22-1549-2022
- 450 Gondwe, M., Krol, M., Gieskes, W., Klaassen, W., & de Baar, H. (2003). The  
 451 contribution of ocean-leaving DMS to the global atmospheric burdens of DMS,  
 452 MSA, SO<sub>2</sub>, and NSS SO<sub>4</sub>= . *Global Biogeochemical Cycles*, *17*(2), n/a–n/a. doi:  
 453 10.1029/2002gb001937
- 454 Grosvenor, D. P., Sourdeval, O., Zuidema, P., Ackerman, A., Alexandrov, M. D.,  
 455 Bennartz, R., ... Quaas, J. (2018). Remote Sensing of Droplet Number  
 456 Concentration in Warm Clouds: A Review of the Current State of Knowl-  
 457 edge and Perspectives [dataset]. *Reviews of Geophysics*, *56*(2), 409–453. doi:  
 458 10.1029/2017RG000593
- 459 Hardacre, C., Mulcahy, J. P., Pope, R. J., Jones, C. G., Rumbold, S. T., Li, C., ...  
 460 Turnock, S. T. (2021). Evaluation of SO<sub>2</sub>, SO<sub>4</sub><sup>2-</sup> and an updated SO<sub>2</sub> dry deposi-  
 461 tion parameterization in the United Kingdom Earth System Model. *Atmospheric*  
 462 *Chemistry and Physics*, *21*(24), 18465–18497. (Publisher: Copernicus GmbH) doi:



- 10.5194/acp-21-18465-2021
- Hersbach, H., Bell, B., Berrisford, P., Hirahara, S., Horányi, A., Muñoz-Sabater, J., ... others (2020). The ERA5 global reanalysis. *Quarterly Journal of the Royal Meteorological Society*, 146(730), 1999–2049. (Publisher: Wiley Online Library)
- Hoesly, R. M., Smith, S. J., Feng, L., Klimont, Z., Janssens-Maenhout, G., Pitkanen, T., ... Zhang, Q. (2018). Historical (1750–2014) anthropogenic emissions of reactive gases and aerosols from the Community Emissions Data System (CEDS). *Geoscientific Model Development*, 11(1), 369–408. Retrieved from <https://www.geosci-model-dev.net/11/369/2018/> (ISBN: 1991-962X) doi: 10.5194/gmd-11-369-2018
- Hoffmann, E. H., Heinold, B., Kubin, A., Tegen, I., & Herrmann, H. (2021). The Importance of the Representation of DMS Oxidation in Global Chemistry–Climate Simulations. *Geophysical Research Letters*, 48(13), e2021GL094068. doi: 10.1029/2021GL094068
- Horowitz, L. W., Naik, V., Paulot, F., Ginoux, P. A., Dunne, J. P., Mao, J., ... Zhao, M. (2020, October). The GFDL Global Atmospheric Chemistry–Climate Model AM4.1: Model Description and Simulation Characteristics. *Journal of Advances in Modeling Earth Systems*, 12(10), e2019MS002032. (Publisher: John Wiley & Sons, Ltd) doi: <https://doi.org/10.1029/2019MS002032>
- Hulswar, S., Simó, R., Gali Tapias, M., Bell, T. G., Lana, A., Inamdar, S., ... Mahajan, A. S. (2022). Third revision of the global surface seawater dimethyl sulfide climatology (DMS-Rev3). *Earth System Science Data*, 14(7), 2963–2987. (Publisher: Copernicus Publications) doi: <https://doi.org/10.5194/essd-14-2963-2022>
- Jarníková, T., & Tortell, P. D. (2016). Towards a revised climatology of summertime dimethylsulfide concentrations and sea–air fluxes in the Southern Ocean. *Environmental Chemistry*, 13(2), 364. doi: 10.1071/EN14272
- Keller, M. D., Bellows, W. K., & Guillard, R. R. (1989). Dimethyl sulfide production in marine phytoplankton. In *Biogenic Sulfur in the Environment* (Vol. 393, pp. 167–182). ACS Symposium Series. Retrieved from <https://doi.org/10.1021/bk-1989-0393.ch011>
- Kirkevåg, A., Grini, A., Olivié, D., Seland, O., Alterskjær, K., Hummel, M., ... Iversen, T. (2018, October). A production-tagged aerosol module for Earth system models, OsloAero5.3 – extensions and updates for CAM5.3–Oslo. *Geoscientific Model Development*, 11(10), 3945–3982. Retrieved from <https://gmd.copernicus.org/articles/11/3945/2018/> (Publisher: Copernicus Publications) doi: 10.5194/gmd-11-3945-2018
- Kloster, S., Feichter, J., Maier-Reimer, E., Six, K. D., Stier, P., & Wetzol, P. (2006). DMS cycle in the marine ocean-atmosphere system—a global model study. *Biogeosciences*, 3(1), 29–51. (Publisher: Copernicus GmbH)
- Korhonen, H., Carslaw, K. S., Spracklen, D. V., Mann, G. W., & Woodhouse, M. T. (2008). Influence of oceanic dimethyl sulfide emissions on cloud condensation nuclei concentrations and seasonality over the remote Southern Hemisphere oceans: A global model study. *Journal of Geophysical Research*, 113(D15). doi: 10.1029/2007jd009718
- Krasting, J. P., John, J. G., Blanton, C., McHugh, C., Nikonov, S., Radhakrishnan, A., ... Zhao, M. (2018). *NOAA-GFDL GFDL-ESM4 model output prepared for CMIP6 CMIP historical [dataset]*. Earth System Grid Federation. Retrieved from <https://doi.org/10.22033/ESGF/CMIP6.8597> doi: 10.22033/ESGF/CMIP6.8597
- Loeb, N. G., Doelling, D. R., Wang, H., Su, W., Nguyen, C., Corbett, J. G., ... Kato, S. (2018, January). Clouds and the Earth’s Radiant Energy System (CERES) Energy Balanced and Filled (EBAF) Top-of-Atmosphere (TOA) Edition-4.0 Data Product [dataset]. *Journal of Climate*, 31(2), 895–918. (Publisher: American Meteorological Society Section: Journal of Climate) doi:

- 10.1175/JCLI-D-17-0208.1
- Mulcahy, J. P., Johnson, C., Jones, C. G., Povey, A. C., Scott, C. E., Sellar, A., ... Andrews, M. B. (2020). Description and evaluation of aerosol in UKESM1 and HadGEM3-GC3. 1 CMIP6 historical simulations. *Geoscientific Model Development*, 13(12), 6383–6423.
- Novak, G. A., Fite, C. H., Holmes, C. D., Veres, P. R., Neuman, J. A., Faloon, I., ... Bertram, T. H. (2021, October). Rapid cloud removal of dimethyl sulfide oxidation products limits SO<sub>2</sub> and cloud condensation nuclei production in the marine atmosphere. *Proceedings of the National Academy of Sciences of the United States of America*, 118(42), e2110472118. doi: 10.1073/pnas.2110472118
- Platnick, S., Meyer, K. G., King, M. D., Wind, G., Amarasinghe, N., Marchant, B., ... Riedi, J. (2017, January). The MODIS cloud optical and microphysical products: Collection 6 updates and examples from Terra and Aqua. *IEEE transactions on geoscience and remote sensing : a publication of the IEEE Geoscience and Remote Sensing Society*, 55(1), 502–525. doi: 10.1109/TGRS.2016.2610522
- Revell, L. E., Kremser, S., Hartery, S., Harvey, M., Mulcahy, J. P., Williams, J., ... Bird, L. (2019). The sensitivity of Southern Ocean aerosols and cloud microphysics to sea spray and sulfate aerosol production in the HadGEM3-GA7. 1 chemistry–climate model. *Atmospheric Chemistry and Physics*, 19(24), 15447–15466.
- Sellar, A. A., Jones, C. G., Mulcahy, J. P., Tang, Y., Yool, A., Wiltshire, A., ... Palmieri, J. (2019). UKESM1: Description and evaluation of the UK Earth System Model. *Journal of Advances in Modeling Earth Systems*, 11(12), 4513–4558.
- Seo, J., Shim, S., Kwon, S.-H., Boo, K.-O., Kim, Y.-H., O'Connor, F., ... Morgenstern, O. (2020, October). The Impacts of Aerosol Emissions on Historical Climate in UKESM1. *Atmosphere*, 11(10), 1095. (Number: 10 Publisher: Multi-disciplinary Digital Publishing Institute) doi: 10.3390/atmos11101095
- Shah, V., Jacob, D. J., Moch, J. M., Wang, X., & Zhai, S. (2020, October). Global modeling of cloud water acidity, precipitation acidity, and acid inputs to ecosystems. *Atmospheric Chemistry and Physics*, 20(20), 12223–12245. (Publisher: Copernicus GmbH) doi: 10.5194/acp-20-12223-2020
- Sheng, J.-X., Weisenstein, D. K., Luo, B.-P., Rozanov, E., Stenke, A., Anet, J., ... Peter, T. (2015). Global atmospheric sulfur budget under volcanically quiescent conditions: Aerosol-chemistry-climate model predictions and validation. *Journal of Geophysical Research: Atmospheres*, 120(1), 256–276. doi: 10.1002/2014JD021985
- Smith, S. J., van Aardenne, J., Klimont, Z., Andres, R. J., Volke, A., & Delgado Arias, S. (2011, February). Anthropogenic sulfur dioxide emissions: 1850–2005. *Atmospheric Chemistry and Physics*, 11(3), 1101–1116. (Publisher: Copernicus GmbH) doi: 10.5194/acp-11-1101-2011
- Tsigaridis, K., Krol, M., Dentener, F. J., Balkanski, Y., Lathière, J., Metzger, S., ... Kanakidou, M. (2006, November). Change in global aerosol composition since preindustrial times. *Atmospheric Chemistry and Physics*, 6(12), 5143–5162. (Publisher: Copernicus GmbH) doi: 10.5194/acp-6-5143-2006
- Turnock, S. T., Allen, R. J., Andrews, M., Bauer, S. E., Deushi, M., Emmons, L., ... Zhang, J. (2020, November). Historical and future changes in air pollutants from CMIP6 models. *Atmospheric Chemistry and Physics*, 20(23), 14547–14579. doi: 10.5194/acp-20-14547-2020
- Turnock, S. T., Butt, E. W., Richardson, T. B., Mann, G. W., Reddington, C. L., Forster, P. M., ... Spracklen, D. V. (2016). The impact of European legislative and technology measures to reduce air pollutants on air quality, human health and climate. *Environmental Research Letters*, 11(2), 024010. (ISBN: 1748-9326) doi: 10.1088/1748-9326/11/2/024010
- Turnock, S. T., Mann, G. W., Woodhouse, M. T., Dalvi, M., O'Connor, F. M.,



- 571 Carslaw, K. S., & Spracklen, D. V. (2019, April). The Impact of Changes in Cloud  
 572 Water pH on Aerosol Radiative Forcing. *Geophysical Research Letters*, 46(7),  
 573 4039–4048. (Publisher: John Wiley & Sons, Ltd) doi: 10.1029/2019GL082067
- 574 Veres, P. R., Neuman, J. A., Bertram, T. H., Assaf, E., Wolfe, G. M., Williamson,  
 575 C. J., . . . others (2020). Global airborne sampling reveals a previously unobserved  
 576 dimethyl sulfide oxidation mechanism in the marine atmosphere. *Proceedings of*  
 577 *the National Academy of Sciences*, 117(9), 4505–4510. (Publisher: National Acad  
 578 Sciences)
- 579 Vogel, A., Alessa, G., Scheele, R., Weber, L., Dubovik, O., North, P., & Fiedler,  
 580 S. (2022). Uncertainty in Aerosol Optical Depth From Modern Aerosol-Climate  
 581 Models, Reanalyses, and Satellite Products. *Journal of Geophysical Research:*  
 582 *Atmospheres*, 127(2), e2021JD035483. doi: 10.1029/2021JD035483
- 583 Walters, D., Baran, A. J., Boutle, I., Brooks, M., Earnshaw, P., Edwards, J., . . .  
 584 Zerroukat, M. (2019). The Met Office Unified Model Global Atmosphere 7.0/7.1  
 585 and JULES Global Land 7.0 configurations. *Geoscientific Model Development*,  
 586 12(5), 1909–1963. doi: 10.5194/gmd-12-1909-2019